

Resonant Inductive Wireless Power Transfer for EV Battery Charging Applications

Master of Technology Phase 1
Project Report

Submitted by
Akash Vishwakarma
(224102101)

Under the Supervision of
Dr. Chandan Kumar



Department of Electronics and Electrical Engineering

Indian Institute of Technology, Guwahati

November, 2023

Abstract

Wireless Power Transfer (WPT) systems transfer electric energy from a source to a load without any wired connection. WPT offers better operational flexibility, safety, and durability in comparison to wired power transfer. Therefore, many applications, such as domestic appliances, mobile robots, mobile phones, and wearable devices, use WPT. WPT is achieved through the inductive coupling between two coils. In WPT methods resonant inductive wireless charging has to gain more attention for medium-high power transfer applications compared to other WPT methods because it exhibits a greater efficiency. Beginning with an evaluation of the individual section parameters and an estimation of the effect of system parameters on performance, the WPT system is designed. Following an analysis of various winding structures, including helix and spiral, and various shapes for the magnetic core, coil coupling was designed. The estimation of values and ratings for the following components has been used in the design of the power supply stages of the WPT system: a) inductors and capacitors that develop resonant coil coupling; b) the power devices such as rectifier and high-frequency (HF) inverter that feed the transmitting coil; and c) the power devices of the converters supplied by the receiver coil: the rectifier diode that feeds the battery in order to optimize the effectiveness of the WPT system.

Contents

1	Introduction	1
1.1	Background	1
1.1.1	WPT System Technology for EVs	3
2	Literature Review	5
2.1	Inductive WPT System	5
Resonant Inductive WPT System	6	
2.1.1	Mono Resonance Compensation Topology	7
Series-Series Topology	7	
Series-Parallel Topology	7	
Parallel-Parallel Topology	8	
Parallel-Series Topology	8	
2.1.2	Multi Resonance Compensation Topology	8
LCL-S Topology	9	
LCL-LCL or Double-Sided LCL Topology	9	
2.2	Motivation and Objectives	10
3	Simulation Results	12
3.1	Open-Loop Simulation of resonant inductive WPT system with LCL-LCL Topology	12
3.1.1	Operation with LCL-LCL Topology at $R_L = 20 \Omega$	13
3.1.2	Operation with LCL-LCL Topology with Battery $E = 50V$	15
4	Hardware Setup and Results	18
4.1	Hardware setup	18
4.1.1	H-Bridge Inverter	18
4.1.2	Diode Bridge Rectifier with DC link Capacitor	19
4.1.3	Coupling Coils and Inductive Parameters	20
4.1.4	Compensation Circuit	21
4.2	Hardware Setup of WPT system	21
4.3	Operating Hardware Setup with LCL-LCL Topology in Open Loop	23

5 Conclusion and Future Work	25
Conclusion	25
Future Work	25

List of Figures

1.1	General scheme of a resonant WPTS.	2
2.1	Scheme of inductive coupling in WPT system.	6
2.2	Mono resonance compensation topologies. (a) Series-Series. (b) Series-Parallel. (c) Parallel-Parallel. (d) Parallel-Series.	8
2.3	Diagram for LCL-S topology.	9
2.4	Diagram for LCL-LCL topology.	10
3.1	Simulation of WPT system with $R_L=20$ ohm.	13
3.2	Operation with LCL-LCL topology at $R_L=20$ ohm. (a) Voltage and current of the transmitter side. (b) Voltage and current of the receiver side.	13
3.3	Output/Load voltage and current waveform when $R_L=20$ ohm.	14
3.4	Simulation diagram of WPTS with $E = 50V$	15
3.5	Operation with LCL-LCL topology at $E = 50V$. (a) Voltage and current of the transmitter side. (b) Voltage and current of the receiver side.	16
3.6	Operation with LCL-LCL topology at $E = 50V$. (a) Voltage across the battery. (b) Current drawn by battery.	16
3.7	State of charge of the battery.	17
4.1	H-Bridge inverter PCB.	19
4.2	Diode-bridge rectifier with dc-link capacitor.	19
4.3	Inductive parameters at $d = 5cm$. (a) $L_T = 49.83 \mu H$. (b) $L_R = 51.46 \mu H$	20
4.4	(a) Compensation inductor. (b) Compensation capacitor.	21
4.5	Hardware architecture of WPT setup.	21
4.6	Complete hardware setup for WPT.	22
4.7	(a) Transmitter coil voltage. (b) Receiver coil voltage. (c) Transmitter coil current. (d) Receiver coil current.	23
4.8	(a) Inverter output voltage. (b) Filter output or primary coil voltage. (c) Load voltage. (d) load current.	24

List of Tables

3.1	Simulation parameters and results.	14
3.2	Simulation parameters and results.	17
4.1	Coil coupling setup measurement.	20
4.2	Hardware specifications and results.	24

Chapter 1

Introduction

Addressing the global concern of climate change, the use of Internal Combustion Engine (ICE) vehicles has raised the need for alternative transportation solutions. Electric vehicles (EVs) powered by renewable energy sources offer a promising solution to reduce reliance on fossil fuels and minimize environmental impact. However, further research and development efforts are required to enhance the performance and autonomy of EVs. This includes advancements in battery technology, utilization of supercapacitors, deployment of fast charging infrastructure, and exploring innovative charging methods such as charging while in motion. Conductive battery chargers, both off-board and on-board, are commonly used to recharge EV batteries. Off-board chargers operate at high power levels to enable quick charging, while on-board chargers facilitate charging at home or charging stations.

1.1 Background

The ongoing focus on these advancements aims to extend the range and efficiency of EVs, promoting their wider adoption as a sustainable transportation option. Two methods of charging EVs are conductive (wired) charging and wireless charging. Conductive charging involves physically connecting the vehicle's charge inlet to an electric supply using cables. While this method is commonly used, it has drawbacks such as messy cords and safety concerns in wet environments [1]. In recent years, there has been a growing interest in providing electric power to vehicles without the need for physical connections to the grid. This has led to the development of WPT systems that enable charging through-field power. Wireless charging of EV batteries offers several

advantages over wired charging, including the elimination of plugs, cables, and outlets, simplified charging procedures, the ability to charge in various settings, and improved convenience. It is expected that WPT system will have a significant impact on the future of EV charging due to these benefits.. WPT systems can be implemented using different technologies based on electric, magnetic, and electromagnetic fields. Among these technologies, Inductive WPT system that utilize magnetic fields are the most practical and efficient.

Inductive WPT system a higher amount of energy per volume compared to electric-field technology and are more effective than electromagnetic technology. Low-power inductive WPT system with closely linked coils have been available for some time. However, there is a growing interest in transmitting medium to high-power electricity over longer distances. Resonant WPT system, also known as inductive WPT system with resonant topology, are widely used for various applications, including wireless charging of EV batteries. Figure 1.1 depicts the general layout of a resonant inductive WPT system.

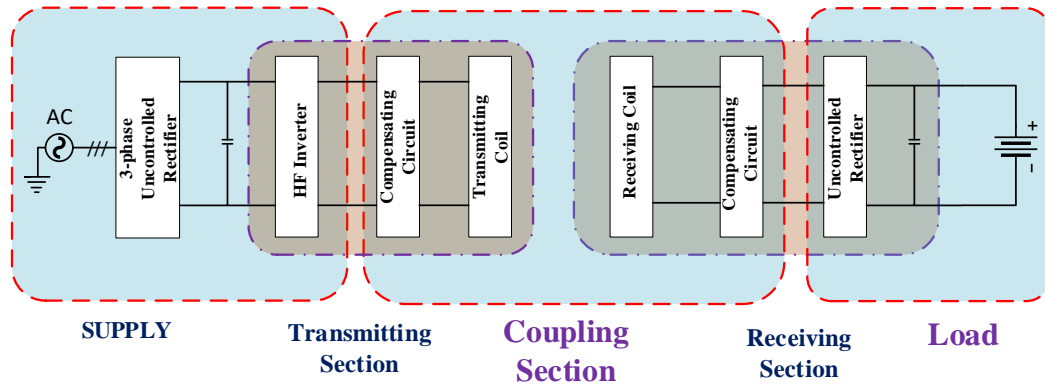


Figure 1.1: General scheme of a resonant WPTS.

The resonant inductive WPT system consists of a transmitting section and a receiving section, each equipped with a coil connected by an air gap. Both sections incorporate power conversion circuitry to facilitate efficient power transfer. In the transmitting section, power is supplied from the grid to the transmitting coil through a high-frequency inverter and a rectifier with an output capacitor. This setup serves as the power source for the transmitting coil, resembling a sinusoidal generator with an added resistance. In the receiving section, the receiving coil induces a voltage, which is rectified using a

diode rectifier with a capacitor. The load of the receiving coil includes the rectifier and battery. With these power conversion circuits, the resonant inductive WPT system enables efficient WPT between the transmitting and receiving coils, allowing convenient charging of the battery pack. Coil alignment is a significant challenge in WPT system applications. During the EV charging process, the alignment between the receiving and transmitting coils may not be perfect due to parking maneuver variations. This misalignment adversely affects power transmission efficiency, resulting in a decreased coupling coefficient compared to aligned conditions. To address these challenges, resonant topology and the use of capacitors are employed. The inductances of the coils are compensated by incorporating capacitors in series or parallel to the coils, tuned to resonate at the supply frequency.

Power electronics circuitry is necessary for the operation of a WPT system. A high-frequency inverter and a high-frequency diode rectifier are components of the power circuitry that supply the transmitting coil. Utilizing new-generation components like SiC/GaN makes it simple to execute high-frequency operations while maintaining a high level of system efficiency. The magnitude of the output voltage of the inverter installed in the transmitting section is used to control the DC voltage across the output capacitor of the rectifier in the receiving section [2].

1.1.1 WPT System Technology for EVs

In the late 1990s, General Motors introduced the EV1 and Chevrolet S-10 EV, which utilized inductive power transfer technology and the Magne Charger (J1773) for wireless charging. These early attempts at wireless charging involved a pad with a primary coil inserted into an EV slot, while the secondary coil was located within the slot. When the pad and slot were combined, a WPT was achieved. However, the performance of these early pads was not satisfactory, as they still required manual engagement and faced similar issues as conventional plug-in charging.

In recent years, with the increasing popularity of e-mobility, significant research has been conducted to make EVs a viable transportation option for the future. WPT charging technology has the potential to positively impact consumer attitudes towards EVs.

While EVs have traditionally faced challenges such as limited driving range and inconvenient charging processes, the introduction of WPT technology for charging can automate and simplify the charging experience for consumers. Additionally, widespread deployment of WPT charging infrastructure can contribute to reducing the size of battery packs, resulting in more efficient EVs. To achieve these benefits, conventional inductive chargers and limited-range WPT charging are not sufficient. Major manufacturers like GM, Qualcomm Halo, Delphi, Toyota, and others have shown interest in wireless charging technology. Qualcomm has recently offered WPT technology for EVs, and various research teams from different institutions are also actively working in this field.

Chapter 2

Literature Review

There are several ways to transfer power wirelessly eg. inductive WPT, capacitive WPT, and radiant WPT. Inductive WPT works on the magnetic field, capacitive WPT works on the electric field and radiant WPT works on electromagnetic waves. This chapter mainly focused on inductive WPT.

2.1 Inductive WPT System

Inductive coupling in WPT system is based on Faraday's law of electromagnetic induction. The system utilizes magnetic fields generated by the current flowing through a wire. When electrical current passes through a wire, it creates a magnetic field that forms a ring shape around the wire. In an inductive WPT system, the alternating voltage applied to one part of the coil results in a different terminal voltage from the corresponding part at the same frequency. The circuit diagram of the inductive coupling WPT system is depicted in Figure 2.1, where L_T and L_R represent the self-inductances of the transmitting and receiving coils, respectively. M denotes their mutual inductance, while R_1 and R_2 indicate the coil resistances [3].

k is the coupling coefficient of the coils. mathematically it can be written as

$$k = \frac{M}{\sqrt{L_T * L_R}} \quad (2.1)$$

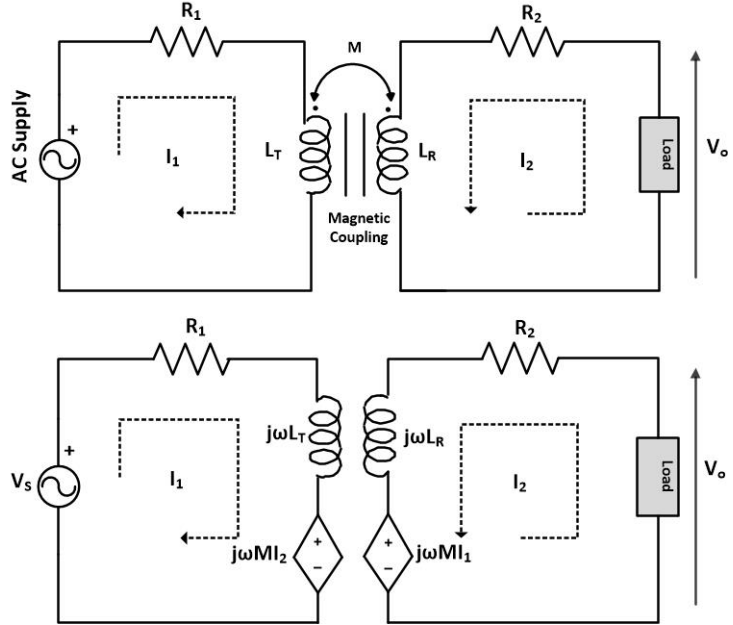


Figure 2.1: Scheme of inductive coupling in WPT system.

Disadvantages of Inductive WPT System

1. Low value of coupling coefficient and mutual inductance.
2. Resistive heating is more.
3. Additionally, it calls for coils and drives electronics, which raises the complexity and expense of manufacture.

Resonant Inductive WPT System

Resonant coupling in WPT system is based on the concept of achieving resonance between L and C components, incorporating capacitors into the coupling coils. Resonant coupling WPT system aim to reduce the required voltage and/or current for power transfer. During resonance, the collapsing magnetic field of the inductor induces an electric current in its windings, which charges the capacitor. Subsequently, the discharging magnetic field of the capacitor generates an electric current that expands the inductor's magnetic field. In this process, the inductor and capacitor exchange equal amounts of mode power [4].

Advantages of resonant inductive WPT system

1. Resonant inductive WPT system is more effective than Inductive WPT system in terms of quality factor and power factor.
2. Can transfer power over a greater distance than inductive WPT system.

Disadvantage of resonant inductive WPT system

1. Power transfer is limited to 1 or 2 meters.

For resonant inductive WPT on the basis of compensation topology it can be categorise into two sub parts:

- Mono resonance compensation topology
- Multi resonance compensation topology

2.1.1 Mono Resonance Compensation Topology

In these topologies only one resonance takes place. There are four basic topologies of mono resonance: series-series (SS), series-parallel (SP), parallel-series (PS), and parallel-parallel (PP). Each topology involves connecting the primary and secondary coils in different configurations with capacitors that are tuned to resonate at the supply frequency [5].

Series-Series Topology

In the series-series topology, both the primary and secondary coils are connected in series with capacitors. The capacitors are adjusted to resonate at the desired operating frequency. Figure 2.2 (a) shows the SS topology.

Series-Parallel Topology

In the series-parallel topology, the primary coil is connected in series with a capacitor, while the secondary coil is connected in parallel with a capacitor. The capacitors are tuned to resonate at the operating frequency. Figure 2.2 (b) shows the SP topology.

Parallel-Parallel Topology

In the parallel-parallel topology, both the primary and secondary coils are connected in parallel with capacitors. The capacitors are adjusted to resonate at the operating frequency. Figure 2.2 (c) shows the PP topology.

Parallel-Series Topology

In the parallel-series topology, the primary coil is connected in parallel with a capacitor, while the secondary coil is connected in series with a capacitor. The capacitors are tuned to resonate at the desired frequency. Figure 2.2 (d) shows PS topology.

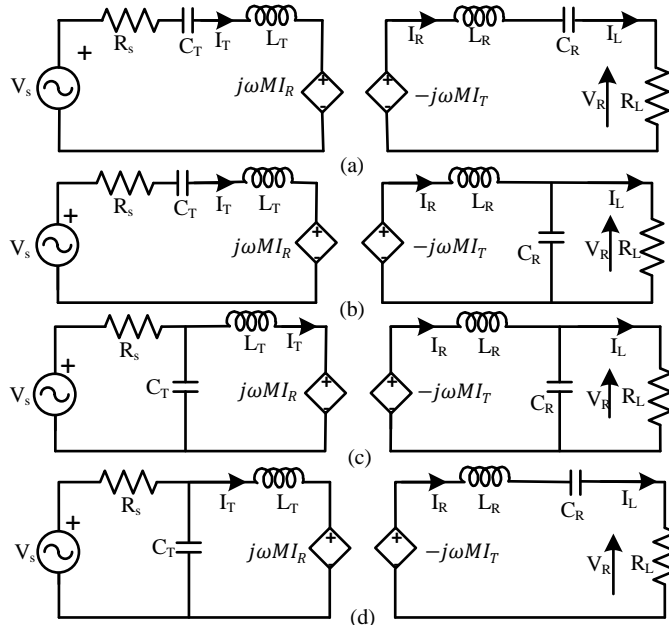


Figure 2.2: Mono resonance compensation topologies. (a) Series-Series. (b) Series-Parallel. (c) Parallel-Parallel. (d) Parallel-Series.

2.1.2 Multi Resonance Compensation Topology

In these topologies more than one resonance takes place. In multi resonance, more than two L and C elements going to be in use. It includes LCL-LCL topology or double-sided LCL topology and LCLS topology.

LCL-S Topology

The LCL-S topology is a configuration commonly used in resonant inductive WPT systems. It consists of two inductors (L_1 , L_T) connected in series with a capacitor (C) placed between them on the primary side. The secondary side only capacitor is connected in series with a coil. Figure 2.3 shows the diagram for LCL-S topology [6]. For LCL-S topology by selection of resonance frequency designing of hardware parameters can be possible. So relation for resonance frequency is

$$\omega_r = \frac{1}{\sqrt{L_1 * C_T}} = \frac{1}{\sqrt{L_T * C_T}} \quad (2.2)$$

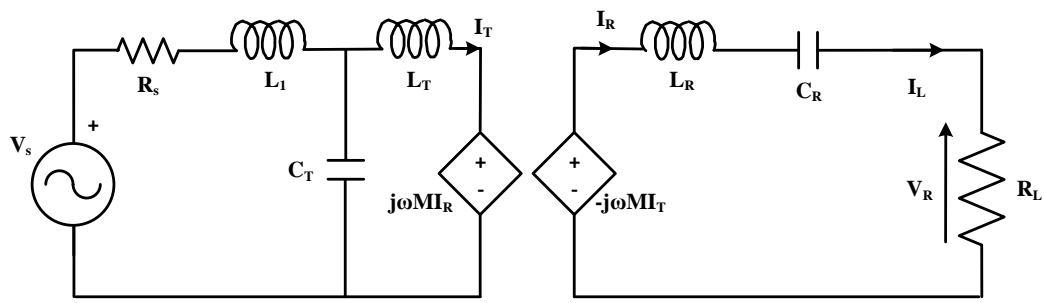


Figure 2.3: Diagram for LCL-S topology.

LCL-LCL or Double-Sided LCL Topology

In the LCL-LCL topology, each LCL network consists of two inductors (L_1 , L_T) connected in series with a capacitor (C) placed between them. The two LCL networks are connected in series, with their capacitor terminals connected together. Figure 2.4 shows the diagram for LCL-LCL topology [7]. For LCL-LCL topology by selection of resonance frequency designing of hardware parameters can be possible. So relation for resonance frequency is

$$\omega_r = \frac{1}{\sqrt{L_1 * C_T}} = \frac{1}{\sqrt{L_T * C_T}} \quad (2.3)$$

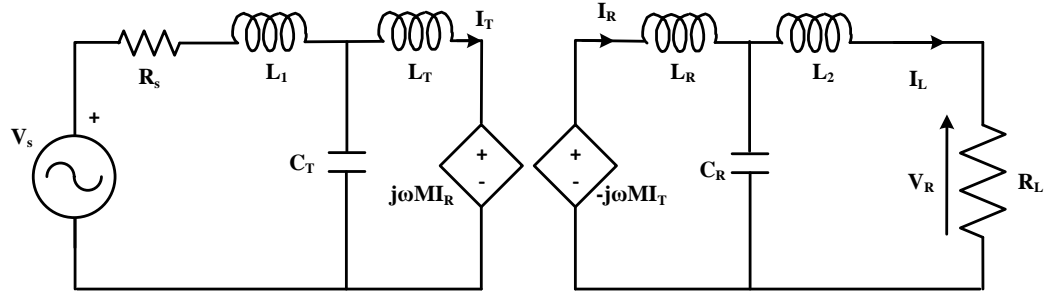


Figure 2.4: Diagram for LCL-LCL topology.

2.2 Motivation and Objectives

Resonant inductive WPT systems have gained significant attention in recent years due to their potential for efficient and contactless power transfer over short to medium distances. This technology offers several advantages over traditional wired power transfer methods, including convenience, flexibility, and enhanced safety. The ability to transfer power wirelessly opens up exciting possibilities for applications such as electric vehicle charging, medical implants, consumer electronics, and smart home devices.

However, despite the promising potential of the resonant inductive WPT system, there are still challenges and limitations that need to be addressed to fully exploit its capabilities. One crucial aspect is maximizing power transfer efficiency. Resonant inductive WPT systems often suffer from losses and reduced efficiency due to factors such as large leakage inductances and reactive elements in the system. These issues can lead to energy wastage, decreased overall system performance, and limited practicality of wireless power transfer technology.

To overcome these challenges, extensive research and development efforts are required to optimize the design and operation of the resonant inductive WPT system. This is where the motivation for this report arises. The objective of this research is to investigate and propose solutions to enhance the efficiency and performance of the resonant inductive WPT system.

All of the above-mentioned points have motivated me to work in the area of inductive WPT with the following work plan:

- Familiarisation with the hardware development process.
- The mathematical design needs to be done to find the parameters of the primary coil, secondary coil, compensators, and high-frequency converter. A further selection of components is to be according to the market availability and designed criteria.
- Tested hardware setup and verified simulation results at lower switching frequency in an open loop.
- Analyse simulation at the higher switching frequency.

Chapter 3

Simulation Results

Simulation analysis is started with open loop simulation of resonant inductive WPT system with LCL-LCL topology is done for hardware purposes. Various results and observations for resistive load and the battery are performed on MATLAB simulink.

3.1 Open-Loop Simulation of resonant inductive WPT system with LCL-LCL Topology

This configuration consists of LCL filters on both the transmitter and receiver sides, contributing to enhanced power transfer efficiency and robustness.

In an open-loop simulation, the behavior and performance of the resonant inductive WPT system are analyzed without incorporating any feedback control. This approach allows for a comprehensive examination of the system's dynamics and characteristics. By utilizing the LCL-LCL topology, the simulation focuses on the inductors (L) and capacitors (C) in the filters, which enable effective filtering and resonance establishment [8].

The LCL-LCL topology offers several advantages. Firstly, it helps in reducing current and voltage stresses across the power electronic devices, enhancing their longevity and reliability. Additionally, this topology aids in mitigating harmonic distortions and improving the power quality of the WPT system. The resonant nature of the LCL-LCL configuration facilitates efficient power transfer by ensuring the impedance of the system is well-matched [9].

3.1.1 Operation with LCL-LCL Topology at $R_L = 20 \Omega$

In this section, simulation results for the LCL-LCL topology with a load resistance of 20Ω , input phase voltage of 100 volts ac and inverter operating at 50kHz switching frequency shown in Figure 3.1.

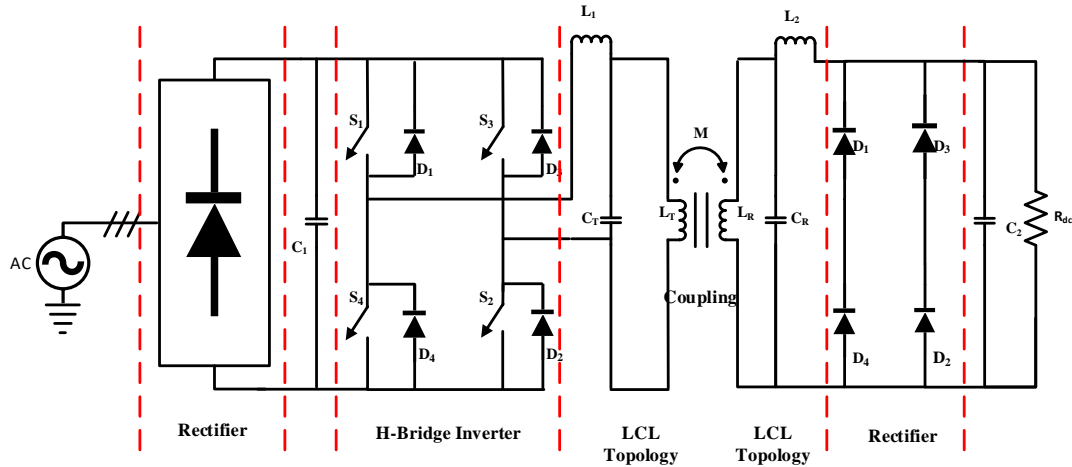


Figure 3.1: Simulation of WPT system with $R_L=20$ ohm.

The transmitter side current is responsible for generating the alternating (AC) magnetic field required for WPT. As depicted in Figure 3.2 (a) waveform shows the variation of voltage and current over time on the transmitter side and (b) waveforms show voltage and current on the receiver side. The magnitude and characteristics of the current are crucial in determining the strength and stability of the magnetic field, which directly affects the efficiency of power transfer to the receiver [8].

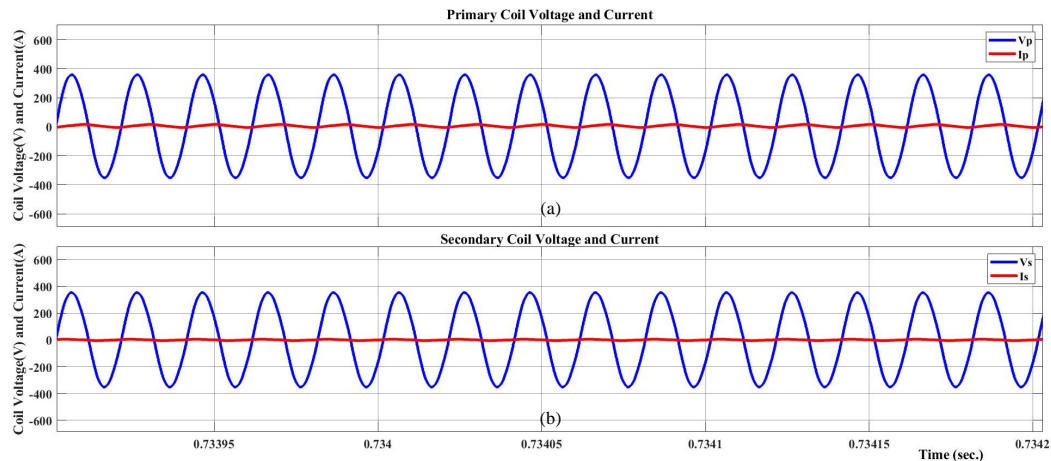


Figure 3.2: Operation with LCL-LCL topology at $R_L=20$ ohm. (a) Voltage and current of the transmitter side. (b) Voltage and current of the receiver side.

On the other hand, the transmitter side voltage represents the voltage supplied by the power source to drive the WPT system. While it is indirectly related to the creation of the magnetic field, it plays a vital role in facilitating the current flow through the transmitter coil or circuitry. The receiver side current corresponds to the current flowing

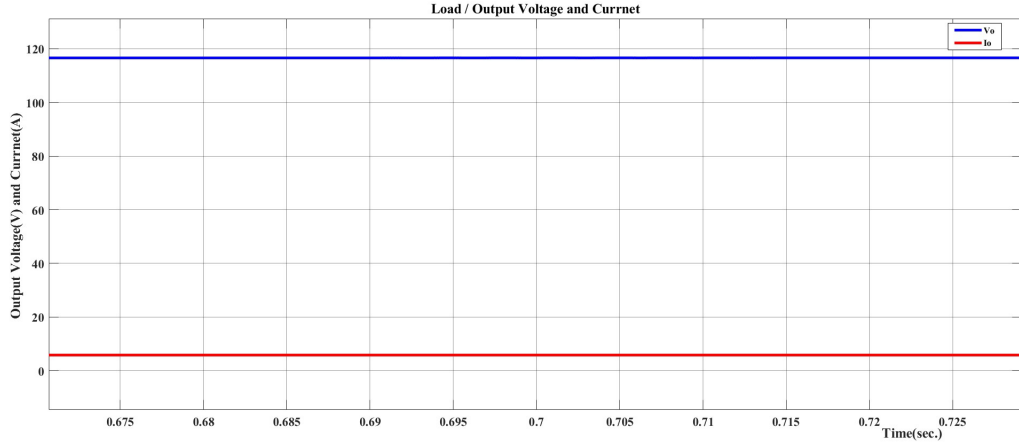


Figure 3.3: Output/Load voltage and current waveform when $R_L=20$ ohm.

through the receiver coil or circuitry. It represents the flow of electrical energy received from the transmitter. In Figure 3.2 (b), the current waveform is shown, indicating its behavior over time. The magnitude and characteristics of the current are significant in determining the power received by the receiver and its ability to deliver that power to the load effectively. Figure 3.3 displays the voltage and current across the load in the LCL-LCL topology with a load resistance of 20 ohms and an input voltage of 100 volts.

Description	Value	Description	Value
$L_1=L_2$	$100 \mu H$	$L_T=L_S$	$100 \mu H$
$C_T=C_S$	$101 \mu F$	Switching frequency	50 kHz
Mutual inductance	$80 \mu H$	Coupling coefficient k	0.8
Input phase voltage	100 V	DC link voltage transmitter	242 V
Primary coil voltage	251 V	Primary coil current	8.6 A
Secondary coil voltage	245 V	Secondary coil current	3.44 A
DC load voltage	108 V	DC load current	5.43 A

Table 3.1: Simulation parameters and results.

The voltage across the load represents the potential difference applied to the load res-

istance. It indicates the electrical energy available at the load for utilization or consumption. In Figure 3.3 the voltage waveform over time is depicted, demonstrating how it varies during the simulation. This voltage waveform provides insights into the behavior of the load voltage and its interaction with the power transfer process. The above table 3.1 shows the simulation parameters and obtained used in simulation [10].

3.1.2 Operation with LCL-LCL Topology with Battery $E = 50V$

Operating the hardware setup when the loading is replaced by a Li-ion battery source of the rating 50V and the capacity of 20Ah shown in Figure 3.4. In this case, maintaining

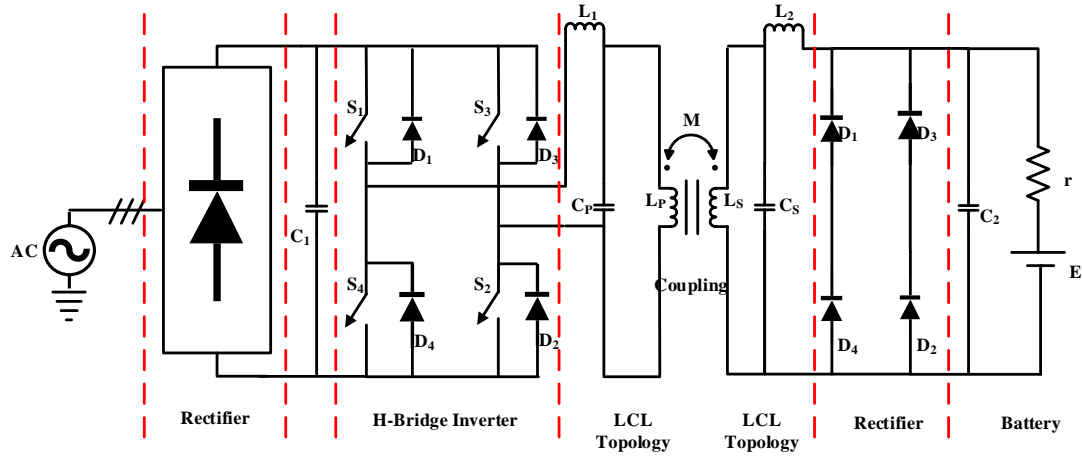


Figure 3.4: Simulation diagram of WPTS with $E = 50V$.

100V phase voltage and switching frequency keeping as 50kHz so the coil waveforms shown below in Figure 3.5.

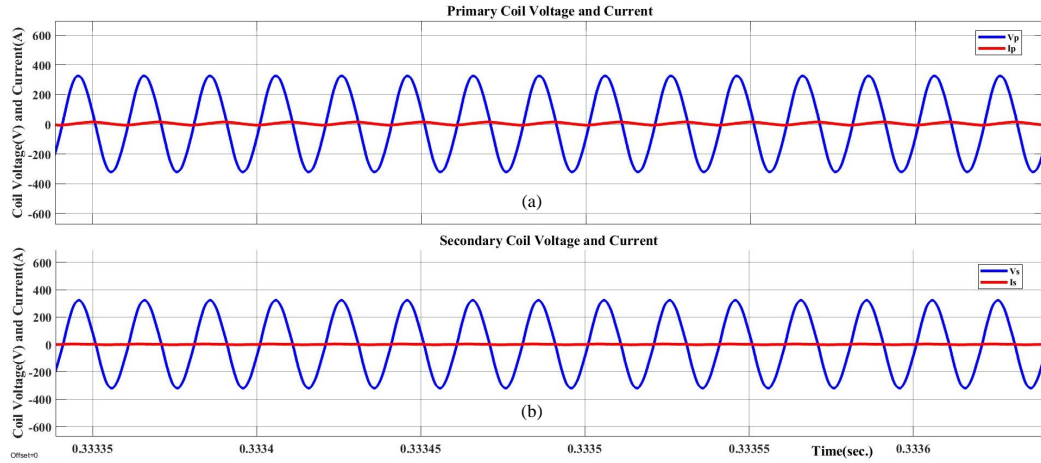


Figure 3.5: Operation with LCL-LCL topology at $E = 50V$. (a) Voltage and current of the transmitter side. (b) Voltage and current of the receiver side.

Receiving side a single-phase diode rectifier is connected which is useful to supply DC load. So the voltage across and current drawn by the battery is shown in Figure 3.6.

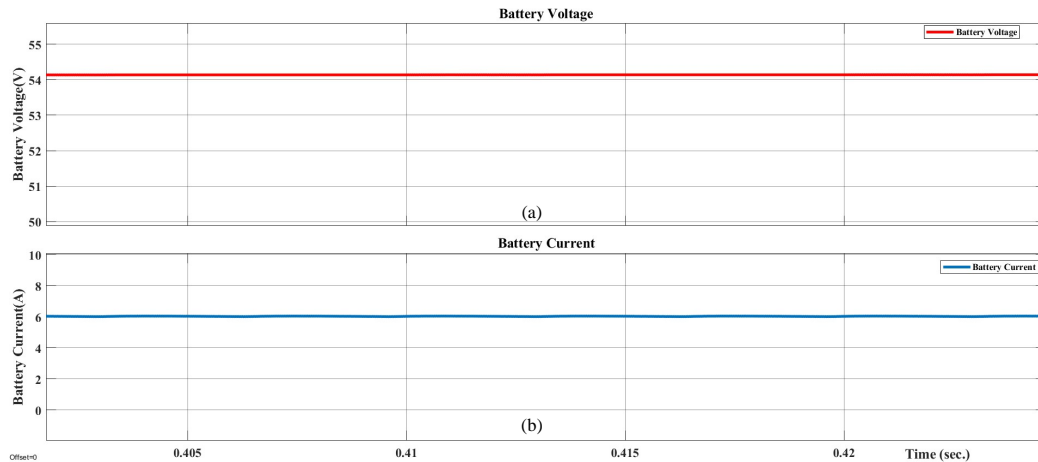


Figure 3.6: Operation with LCL-LCL topology at $E = 50V$. (a) Voltage across the battery. (b) Current drawn by battery.

Observing the state of the charge of the battery when it draws constant current from the DC link on the receiver side is shown in Figure 3.6. Initially, the state of charge is 50% and it increases linearly with time shown in Figure 3.7.

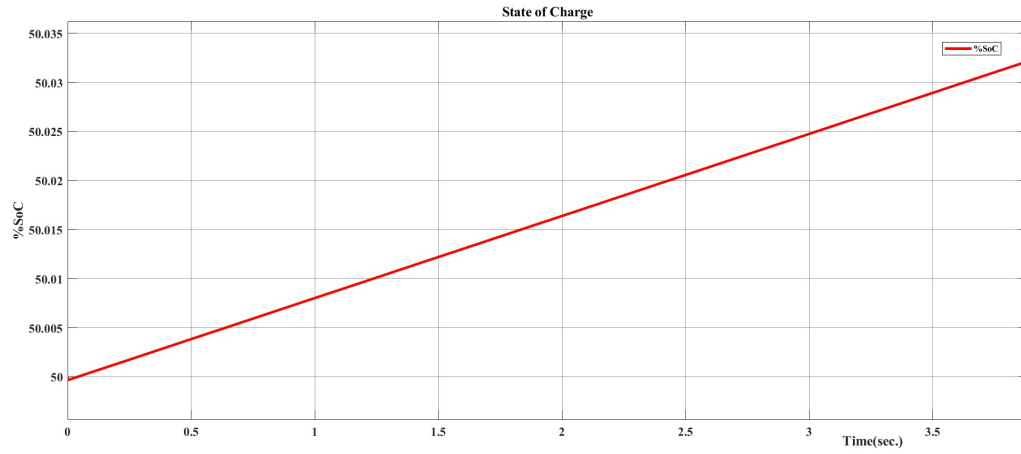


Figure 3.7: State of charge of the battery.

Below table 3.2 shows the simulation parameters and results during the charging of the battery. From this simulation a constant power of 319.78W is delivering to the battery.

Description	Value	Description	Value
Input phase voltage	100 V	DC link voltage transmitter	242 V
Primary coil voltage	226 V	Primary coil current	8.47 A
Secondary coil voltage	223 V	Secondary coil current	1.72 A
DC load voltage	54.2 V	DC load current	5.9 A

Table 3.2: Simulation parameters and results.

Chapter 4

Hardware Setup and Results

This chapter focuses on the application of the power electronics circuits and coil coupling methods for WPT system covered in the preceding chapters. First, a discussion is had on the method and measurement of spiral coil coupling along with the measurement of inductive characteristics and magnetic flux density. The power electronics setup is then presented together with the coil system. Both systems were finally integrated, and a number of measurements were taken under various load conditions.

4.1 Hardware setup

4.1.1 H-Bridge Inverter

The PCB of the H-bridge inverter incorporates several essential circuits that contribute to the efficient and safe operation of the inverter. These circuits include (a) Blanking Circuit: Providing 50 μ sec. blanking time between the operation of switches of the same leg. (b) Protection Circuit: Providing over and under voltage protection from the input side. (c) Gate Driver Circuit: The main purpose to give gate signals to switches with appropriate blanking time. (d) Power Circuit: For converting DC signal in the form of AC.

The PCB layout of the H-bridge inverter is useful to convert DC voltage to AC voltage. By changing the switching frequency we can operate it as the desired fundamental frequency. PCB of the H-bridge inverter plays a critical role in providing the necessary control, protection, and power delivery for the resonant inductive WPT system. Figure 4.1 shows the H-bridge inverter PCB.



Figure 4.1: H-Bridge inverter PCB.

4.1.2 Diode Bridge Rectifier with DC link Capacitor

A 3-phase and a single-phase diode bridge rectifier are used at the transmitter side and receiver side respectively. The 3-phase rectifier is directly connected to the grid and acts as input for dc-ac converter. DC link capacitors are used to reduce ripple on the output of the diode bridge rectifier. The output capacitor of the rectifier has a capacity of 1.88mF and a rating of 400V. At the receiver side, the output capacitor of the rectifier has a capacity of 4.7 mF and a rating of 450 V. Figure 4.2 shows the diode bridge rectifier with a dc-link capacitor.

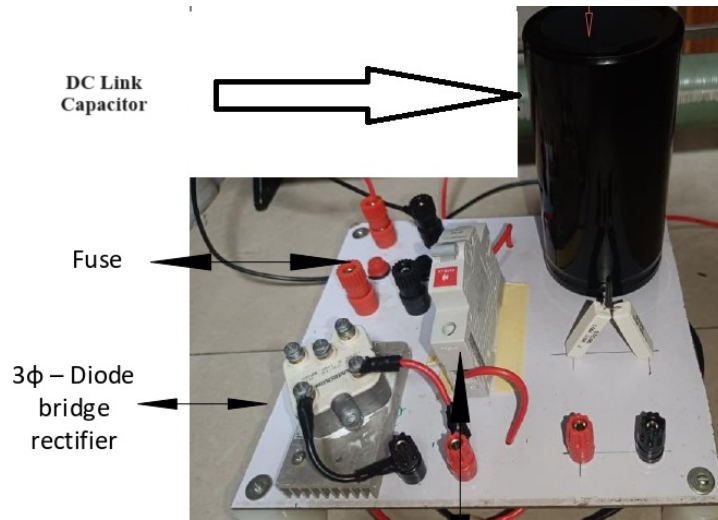


Figure 4.2: Diode-bridge rectifier with dc-link capacitor.

4.1.3 Coupling Coils and Inductive Parameters

Copper Litz wire by maintaining the appropriate distance between turns which minimizes skin and proximity effects, improving current distribution and reducing power losses. The inductive parameters of the coils have been measured by using an LCR meter. By measuring the self-inductance L_{ser} at the terminals of the series connection of the two coils, the mutual inductance can be calculated. Figure 4.3 shows the measured parameters of the coils through an LCR meter.

Then from the expression M will specified,

$$L_{series} = L_T + L_R + 2M \quad (4.1)$$

k is derived as

$$k = \frac{M}{\sqrt{L_T * L_R}} \quad (4.2)$$

Coil distance	L_T	L_R	M	k
0.05 m	49.829 μ H	51.462 μ H	24.24 μ H	0.48
0.1 m	45.829 μ H	47.462 μ H	15.03 μ H	0.322

Table 4.1: Coil coupling setup measurement.

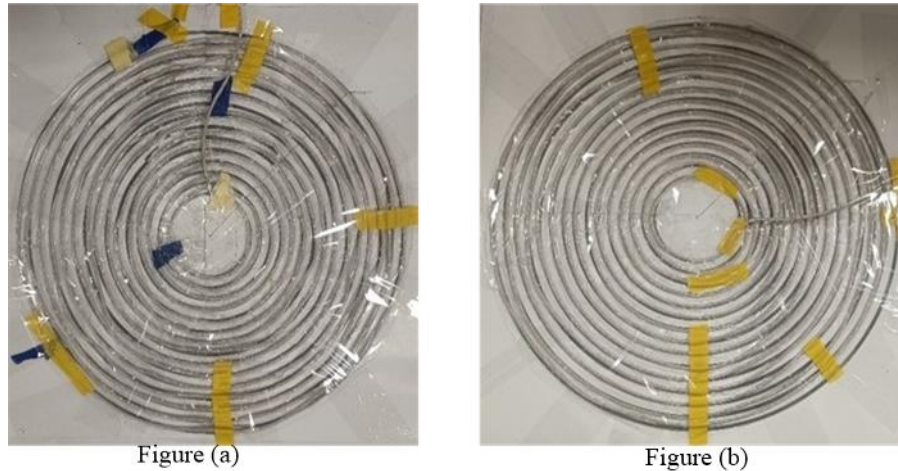


Figure 4.3: Inductive parameters at $d = 5\text{cm}$. (a) $L_T = 49.83 \mu\text{H}$. (b) $L_R = 51.46 \mu\text{H}$.

4.1.4 Compensation Circuit

The LCL-LCL compensation circuit consists of two inductors as of inductances of both coils and two resonance capacitors made by connecting 12 capacitors in parallel [8]. Each capacitor has a capacity of $0.47 \mu\text{F}$ and supports a voltage of about 200 V to a working frequency of 10 kHz. The designed inductors ($L_1=47.8 \mu\text{H}$ and $L_2=49.2 \mu\text{H}$) and capacitors ($C_P=5.22 \mu\text{F}$ and $C_S=5.06 \mu\text{F}$) are shown in Figure 4.4.

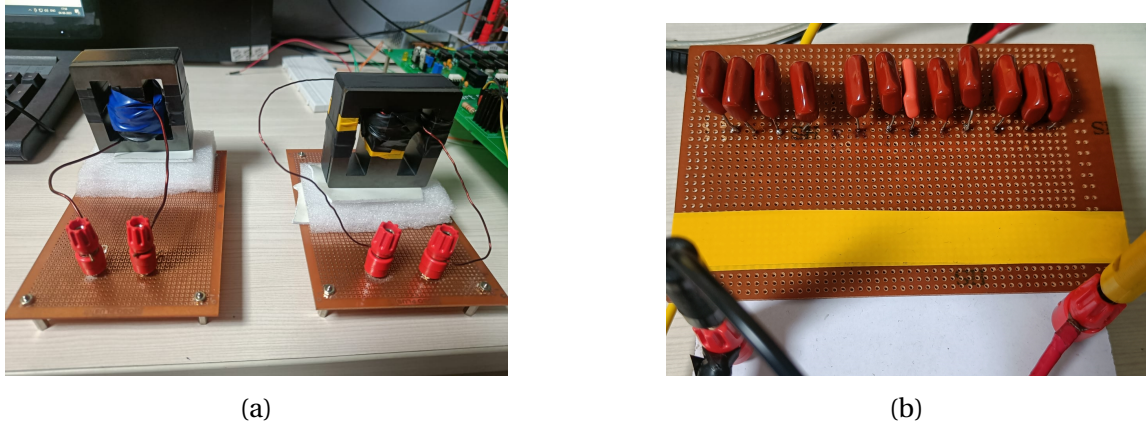


Figure 4.4: (a) Compensation inductor. (b) Compensation capacitor.

4.2 Hardware Setup of WPT system

Figure 4.5 shows the hardware architecture of a resonant inductive WPT system with LCL-LCL topology.

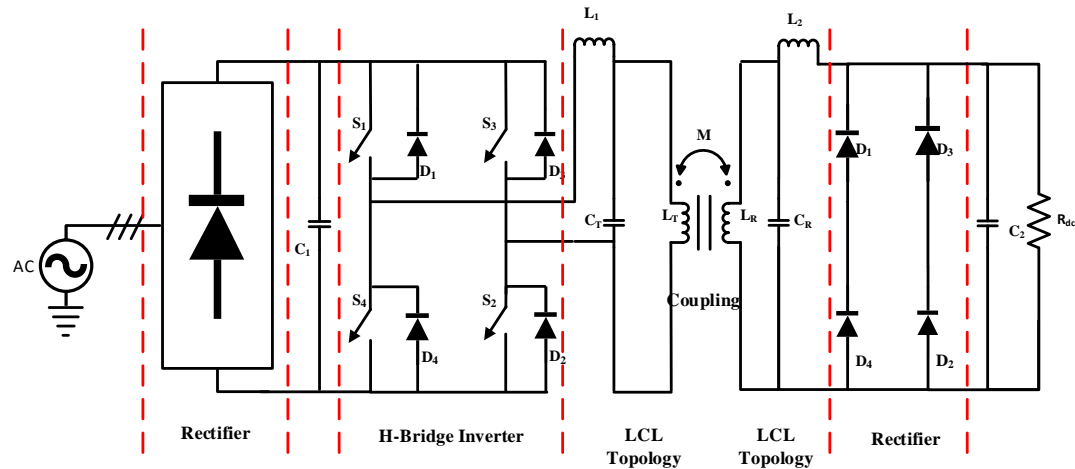


Figure 4.5: Hardware architecture of WPT setup.

This configuration consists of a primary (transmission) side and a secondary (receiver) side. On the primary side, an AC power source is converted into a high-frequency AC signal using a combination of a diode bridge rectifier and a high-frequency inverter. This signal is then fed into the primary resonant coil, generating a magnetic field. The secondary side comprises a resonant coil that receives the magnetic field and the signal then passes through LCL and is given as an input to the diode bridge rectifier which converts this ac signal into a pulsating DC, the dc voltage passes through the dc link capacitor and fed to load. The energy is rectified and used to power the load or charge a battery. Complete hardware setup with resistive load is shown in figure 4.6.

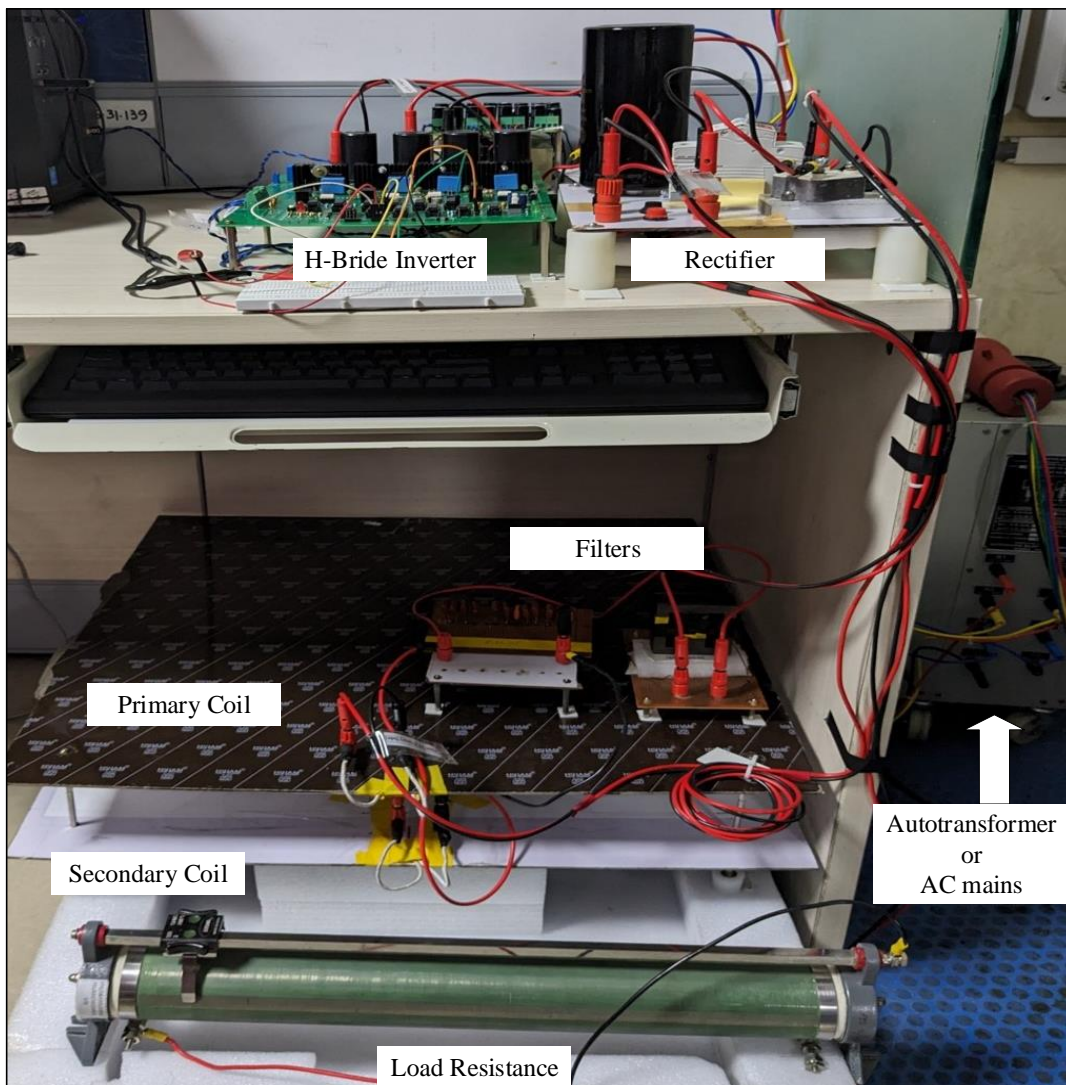


Figure 4.6: Complete hardware setup for WPT.

4.3 Operating Hardware Setup with LCL-LCL Topology in Open Loop

This section presents the hardware testing results of the resonant inductive WPT system with the LCL-LCL topology. The system was tested under various input voltage conditions, with a load resistance of 20 ohms connected to the secondary side. In this section, the hardware results of the resonant inductive WPT system with the LCL-LCL topology are presented. The system was tested under specific operating conditions, with phase voltage (V_{in}) of 9.5 V the distance between two coils is 0.05 m. The output power of the system was measured to be 20.79 Watts. Figure 4.8 (a) and (b) illustrate the voltages across the transmitter and receiver coils respectively. These waveforms represent the transferred power from the transmitter to the receiver side of the system.

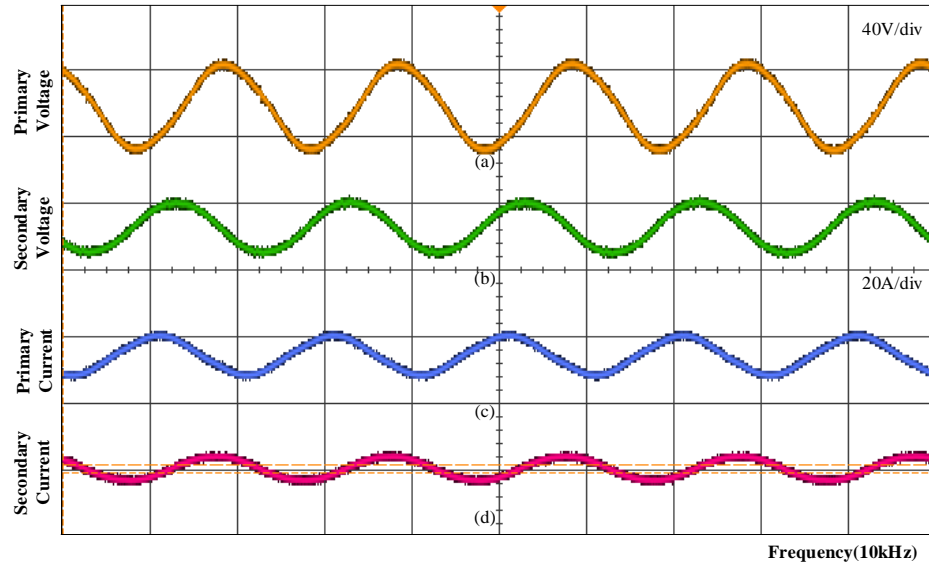


Figure 4.7: (a) Transmitter coil voltage. (b) Receiver coil voltage. (c) Transmitter coil current. (d) Receiver coil current.

In below Figure 4.8 showcases the hardware results (a) Inverter output voltage switching provided by signal generator, (b) Filter output or primary coil voltage, (c) Load voltage and (d) load current The hardware results provide valuable insights into the performance and efficiency of the resonant inductive WPT system with LCL-LCL topology under different input voltage conditions. The observed waveforms and power measurements are shown by maintaining 9.5V phase voltage and 20V DC link voltage.

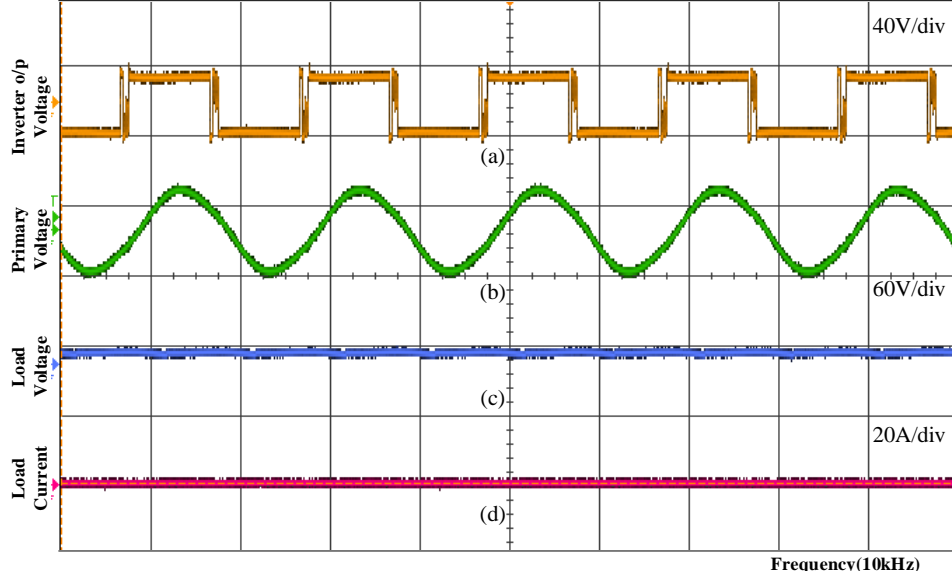


Figure 4.8: (a) Inverter output voltage. (b) Filter output or primary coil voltage. (c) Load voltage. (d) load current.

Description	Value	Description	Value
Distance between coils	5cm	Switching frequency	10kHz
Phase voltage	9.5V	DC Link Voltage	20V
Primary Coil Voltage	22.5V	Secondary Coil Voltage	19.7V
Avg. Output Voltage	18.9	Avg. Output Current	1.1A
Output Power	20.79W		

Table 4.2: Hardware specifications and results.

The analysis of the voltage and current waveforms across the transmitter and receiver coils allows for an assessment of the system's performance, power transfer capability, and overall efficiency. These results aid in validating the effectiveness of the LCL-LCL topology for WPT and provide valuable insights for future enhancements and optimizations of the system.

Chapter 5

Conclusion and Future Work

Conclusion

This report focuses on the operation and simulation of the resonant inductive WPT system using LCL-LCL topology. This report investigates the open-loop operations of the resonant inductive WPT system for LCL-LCL topology. These operations are modeled and successfully simulated in the Simulink environment. Various observations and findings are thoroughly documented in this project report. The coil layout is tested at different heights to observe its coupling coefficient and mutual inductance.

Future Work

The successful completion of this report on the resonant inductive WPT system opens up several avenues for future work and development. The following are potential areas for future work:

1. Efficiency Enhancement: Efforts can be made to further enhance the efficiency of the resonant inductive WPT system. This involves investigation and mitigates the losses.
2. Enhancement in Magnetic Coupling: By changing the permeability of the medium enhancement of the coupling is possible.
3. Operation at High Switching Frequency: By increasing the switching frequency, filter size will be reduced and more power transfer can be achieved.

4. Analyse the inductive WPT: In this section analyze the inductive WPT from transmitter side to receiver side using Ansys Maxwell.
5. Operation in Closed Loop: The output power of resonant inductive WPT is needed to follow the reference setpoint. It requires to operate the system in closed loop for achieving the desired output.

Bibliography

- [1] C. C. Chan, “The state of the art of electric, hybrid, and fuel cell vehicles,” *Proceedings of the IEEE*, vol. 95, no. 4, pp. 704–718, 2007.
- [2] H. Chen, X. Wang, and A. Khaligh, “A single stage integrated bidirectional ac/dc and dc/dc converter for plug-in hybrid electric vehicles,” in *2011 IEEE Vehicle Power and Propulsion Conference*, no. 11, 2011, pp. 1–6.
- [3] H. Abe, H. Sakamoto, and K. Harada, “A noncontact charger using a resonant converter with parallel capacitor of the secondary coil,” *IEEE Transactions on Industry Applications*, vol. 36, no. 2, pp. 444–451, 2000.
- [4] S. Song, W. Zhang, Z. Jin, and Q. Geng, “Analysis of s-s resonance compensation circuit of electric vehicle wireless power transfer system,” in *2020 IEEE 4th Conference on Energy Internet and Energy System Integration (EI2)*, 2020, pp. 619–622.
- [5] E. Ayisire, A. El-Shahat, and A. Sharaf, “Magnetic resonance coupling modelling for electric vehicles wireless charging,” in *2018 IEEE Global Humanitarian Technology Conference (GHTC)*, 2018, pp. 1–2.
- [6] S. Sasikumar and K. Deepa, “Comparative study of lcl-s and lcc-s topology of wireless ev charging system,” in *2019 Innovations in Power and Advanced Computing Technologies (i-PACT)*, vol. 1, 2019, pp. 1–6.
- [7] Y. G. H. L. G. C. Chuang Liu, Shukun Ge, “Double-lcl resonant compensation network for electric vehicles wireless power transfer: experimental study and analysis,” vol. 1, 2016, pp. 1–8.
- [8] M. Khalilian and P. Guglielmi, “A hybrid topology wireless power transfer system with constant current or constant voltage output for battery charging application,”

in *2019 AEIT International Conference of Electrical and Electronic Technologies for Automotive (AEIT AUTOMOTIVE)*, 2019, pp. 1–6.

- [9] A. Mahesh, B. Chokkalingam, and L. Mihet-Popa, “Inductive wireless power transfer charging for electric vehicles—a review,” *IEEE Access*, vol. 9, pp. 137 667–137 713, 2021.
- [10] A. P. Sample, D. T. Meyer, and J. R. Smith, “Analysis, experimental results, and range adaptation of magnetically coupled resonators for wireless power transfer,” *IEEE Transactions on Industrial Electronics*, vol. 58, no. 2, pp. 544–554, 2011.